Identification of 5-Hydroxycotinine in the Plasma of Nicotine-Treated Mice: Implications for Cotinine Metabolism and Disposition in Vivo[S]

[ID] Keiko Kanamori, Syed M. Ahmad, Chang Sung Shin,[1] Abdul Hamid, and [ID] Kabirullah Lutfy

Department of Pharmaceutical Sciences, College of Pharmacy, Western University of Health Sciences, Pomona, California (K.K., S.M.A., C.S.S., A.H., K.L.) and Lab Launch, Monrovia, California (K.K.)

ABSTRACT

Two oxidation products of cotinine, 5-hydroxycotinine (5-HC) and cotinine N-oxide (CNO), were identified for the first time in vivo in the plasma of C57BL/6 mice after injection of nicotine (1 mg/kg) or exposure to an e-cigarette (e-cig) containing 2.4% nicotine. Liquid chromatography–mass spectrometry was used to separate 3-hydroxycotinine (3-HC), 5-HC, and CNO and to quantify each by the sensitive direct detection of their parent ion with m/z of 193.097. In nicotine-injected mice, 5-HC was as abundant as 3-HC 15 minutes postinjection, and CNO was readily detectable. In e-cig–exposed mice with plasma nicotine levels resembling those of human smokers, plasma 5-HC and CNO, as well as 3-HC, were readily quantifiable at the end of the 4-hour exposure time. In nicotine-injected mice, the combined concentration of 3-HC plus 5-HC plus CNO, all formed from cotinine by CYP2A5, was higher ($P < 0.01$) in females than in males, although the male-female difference in cotinine plasma level did not reach statistical significance. The result highlights the importance of considering these three oxidation products of cotinine in examining cotinine metabolism and disposition. Coumarin 7-hydroxylase activity, a specific marker of CYP2A5, measured in the hepatic microsomes of untreated mice showed that females have higher activity ($P < 0.001$) than males ($N = 8$ per sex). The abundance of plasma 5-hydroxycotinine in nicotine-treated mice raises intriguing questions about the site of its origin (hepatic or possibly kidney CYP2A5) and the routes of its disposition because urinary excretion of 5-HC has not been detected by liquid chromatography with tandem mass spectrometry in mice and is controversial in human smokers.

SIGNIFICANCE STATEMENT

Nicotine is the active ingredient of tobacco, but its elimination route through its biomarker cotinine is not fully understood. By liquid chromatography–mass spectrometry, this study has identified and quantified for the first time 5-hydroxycotinine and cotinine N-oxide, which are oxidation products of cotinine, in the plasma of mice treated with nicotine or exposed to e-cigarettes. The results raise intriguing questions about nicotine disposition in vivo in this well established preclinical model of human smokers.

Introduction

Nicotine is the primary component of cigarettes and is responsible for developing addictive behaviors. Nicotine is metabolized to cotinine by CYP2A6 in humans (Cashman et al., 1992; Nakajima et al., 1996; Messina et al., 1997; Murphy et al., 1999) and CYP2A5 in mice (Murphy et al., 2005; Siu et al., 2006; Zhou et al., 2010). These two enzymes are very similar in tissue distribution (Su and Ding, 2004) and in amino acid sequences (84%) (Murphy et al., 2005). Hence, the mouse is an excellent animal model for studying the metabolic pathways and pharmacological effects of nicotine. Our recent studies examined the role of pituitary adenylyl cyclase activating polypeptide in nicotine self-administration (Tseng et al., 2019) and anxiety-like behaviors associated with nicotine withdrawal in mice (Nega et al., 2020). There were male/female differences in the role of pituitary adenylyl cyclase activating polypeptide in affective signs of nicotine withdrawal (Nega et al., 2020). Likewise, we discovered male/female differences in nicotine-stimulated corticosterone secretion (Nguyen et al., 2020). The rise in corticosterone was further increased in male but not female mice after repeated nicotine treatment (Nguyen et al., 2020). Furthermore, we observed that the level of cotinine, a biomarker of nicotine use, was increased to a greater extent in female than male mice (Nguyen et al., 2020). However, it is unknown if cotinine's metabolic pathway would be different between male and female mice.

Cotinine is oxidized by CYP2A5 to *trans* 3′-hydroxycotinine (*trans* 3-HC), 5′-hydroxycotinine (5-HC), and cotinine N-oxide (CNO) (Fig. 1). In mouse plasma, *trans* 3-HC was detected after injection of cotinine (1 mg/kg) (Siu and Tyndale, 2007). 5-HC was identified in vitro upon incubation of recombinant human CYP2A6 with hamster liver microsome and cotinine (Murphy et al., 1999), and CNO upon incubation of primary

ABBREVIATIONS: 3-HC, 3-hydroxycotinine; 5-HC, 5-hydroxycotinine; CNO, cotinine N-oxide; COT, cotinine; E-cig, e-cigarette; LCMS, liquid chromatography–mass spectrometry; LC-MS/MS, liquid chromatography with tandem mass spectrometry; MS, mass spectrometry; WT, wild-type.
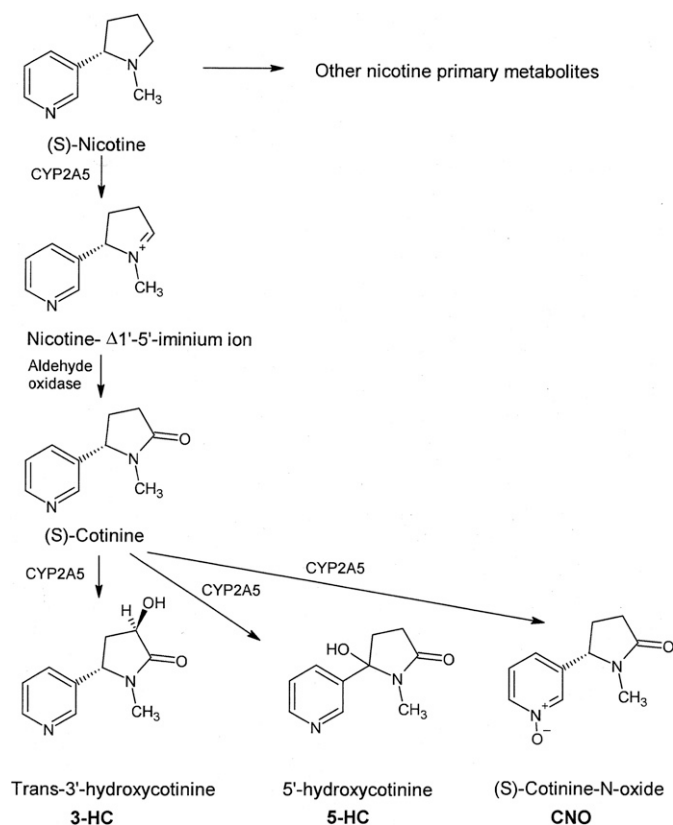
Fig. 1. Metabolic pathways of nicotine to cotinine and to its oxidation products *trans* 3-HC, 5-HC, and CNO catalyzed by CYP2A5 (prepared with ACD Chemsketch software).

mouse hepatocyte culture with ^{14}C-cotinine (Foth et al., 1992). However, 5-HC and CNO have not been detected in vivo in the plasma of mice after nicotine administration. In nicotine-treated mice, the major urinary elimination product was 3-hydroxycotinine (3-HC) (77%), followed by CNO (16%), whereas cotinine represented only 3%–4% (Raunio et al., 2008). In human smokers, 5-HC is considered as a possible urinary product (Murphy, 2021) because its concentration has only been reported in a review article (Neurath, 1994). Accordingly, there is a knowledge gap in the identity and quantity of cotinine oxidation products that are formed in the liver, released into circulation, reabsorbed, and undergo renal elimination. These oxidation reactions in liver microsomes are accompanied by the release of reactive oxygen species, which can cause oxidative stress; this, in turn, is thought to play an important role in the regulation of CYP2A5 (Abu-Bakar et al., 2013). Hence, it is important to characterize these oxidation products of cotinine and their possible effect on CYP2A5. Thus, our first aim is to identify and quantify oxidation products of cotinine in vivo in the plasma of nicotine-treated mice.

Previous studies of CYP2A5 and its role in nicotine metabolism have focused mainly on male mice. This is due to some characteristics of female CYP2A5 that have hampered its determination in females. Female CYP2A5 protein is indistinguishable in western blot from female-specific CYP2A4 protein, which has 98% identity in amino acid sequence to CYP2A5 but contributes little to nicotine metabolism in vivo (Murphy et al., 2005). Consequently, there is sparse information on how CYP2A5-catalyzed nicotine metabolism differs between female and male mice. As stated above, we have recently reported the first quantitative data on male-female differences in nicotine-induced elevation of plasma cotinine (Nguyen et al., 2020). As the first step toward

understanding the role of CYP2A5 in the observed sexual dimorphism, our second aim is to measure coumarin 7-hydroxylase activity as a specific marker of CYP2A5 activity (Raunio et al., 2020) in the liver microsome of male and female C57BL/6 mice.

Recent studies of nicotine metabolites in the body fluids of rodents have used liquid chromatography with tandem mass spectrometry (LC-MS/MS) (Murphy et al., 1999; Siu and Tyndale, 2007; Raunio et al., 2008; Li et al., 2012). After separation by liquid chromatography, each metabolite undergoes collision-induced fragmentation to characteristic product ions, which are quantified by comparison with standards. Although the method is highly selective, sensitivity can be reduced by the fragmentation process and choice of the fragment ion. For quantifying metabolites present in the plasma on the order of $\sim$0.1 nmol/mL and where sample volume is limited as in mouse plasma, a sensitive assay method is desirable. We report here the separation of 3-HC, 5-HC, and CNO by their different retention times and quantification of the parent ions of 3-HC, 5-HC, and CNO by direct high-resolution mass spectrometry (MS).

Materials and Methods

Chemicals. (-)-Cotinine was purchased from Cayman Chemical (Ann Arbor, MI). *Trans* 3-hydroxycotinine (1 mg/mL in methanol), *trans* 3-hydroxycotinine-d_3 (0.1 mg/mL in methanol), ($\pm$)-cotinine-d_3, coumarin, 7-hydroxycoumarin, and Bradford reagents were purchased from Millipore Sigma (St. Louis, MO). 5-Hydroxycotinine (N-methyl 2-oxo 3-pyridinebutanamide) was purchased from Santa Cruz Biotechnology (Dallas, Texas). (S)-Cotinine N-oxide and (R, S)-cotinine-d_3 N-oxide were purchased from Toronto Research Chemicals (Toronto, Canada). Microsome isolation kit (BioVision K249-50) was purchased from Abcam (Milpitas, CA).

Animal Studies. A total of 37 male and 30 female C57BL/6J mice (24–48 g), bred in-house, were used at the age of 2–8 months. All experiments were carried out according to the National Institutes of Health guidelines for the proper care and use of animals in research and approved by the Institutional Animal Care and Use Committee (R20/IACUC/008 and R21/IACUC/009) at the Western University of Health Sciences (Pomona, CA).

Nicotine Injection. The procedure has been described in detail previously (Nguyen et al., 2020). Briefly, mice were brought to the laboratory and allowed to habituate to the test room for 1 hour. For the single-dose study, mice were then injected with saline or nicotine (1 mg/kg; $N = 5$ to 6 mice per group/sex). Fifteen minutes later, mice were euthanized by cervical decapitation with a pair of sharp scissors, and trunk blood was collected in tubes containing 7% EDTA. Blood samples were then spun (14,000 rpm) for 10 minutes, and supernatant was collected and stored at $-80°C$ until use. For the repeated-dose study, mice were treated with saline or nicotine (1 mg/kg s.c.; $N = 4$–6 mice per treatment and sex) once daily for 6 consecutive days. On day 7, the mice were injected with nicotine (1 mg/kg), followed by blood collection 15 minutes later as described above.

E-Cigarette Treatment. Male C57BL/6J mice were brought to the laboratory and habituated to the room for 1 hour. Mice were then exposed to an e-cig (e-cigarette) containing zero or 2.4% nicotine for 4 hours (from 10:00 to 14:00). The e-cig system, EcigAero manufactured by AutoMate Scientific, Inc. (Berkeley, CA), described previously (Shao et al., 2019), was used with the following protocol in our laboratory at the Western University of Health Sciences. It was programmed to generate e-cig aerosol exposure, i.e., ten puffs per hour, with a puff duration of 4 seconds and interpuff interval of 10 seconds, using classic tobacco flavor bluCig PLUS e-cig tanks. Mice were euthanized 5 to 6 minutes after the 4-hour exposure period, and the trunk blood was collected in 1.5-ml vials containing 50 μL of a 7% EDTA solution. The vials were then spun for 10 minutes at 14,000 rpm at 4°C. Plasma samples were collected and stored at $-80°C$ until analysis.

Liquid Chromatography–Mass Spectrometry. The analyses were performed on an Acquity Ultra-Performance Liquid-Chromatography system coupled to a Xevo ToF mass spectrometer (Waters Corporation, Milford, MA) located in the Water and Environment Laboratory at California Institute of Technology. Chromatographic separations of 3-HC, 5-HC, and CNO were achieved

on an Acquity BEH HILIC column using the same mobile phases and the gradient program as described in detail previously for nicotine and cotinine measurements (Nguyen et al., 2020). The mass spectrometer was operated in the positive electrospray ionization mode. The liquid chromatography–mass spectrometry (LCMS) chromatograms of *trans* 3-HC, 5-HC, and CNO were acquired by selection for $[M+H]^+$ with m/z of 193.0977 with a mass window of ±0.01 Da because CNO has the same mass as 3-HC and 5-HC. Those for *trans* 3-HC-d_3 and CNO-d_3 were acquired by selection for $[M+H]^+$ with m/z of 196.1162 and 196.1178, respectively, with the same mass window. MassLynx software (v. 4.1) was used for data acquisition and analyses.

Preparation of Standards. The stock solutions of 3-HC and 5-HC were serially diluted in methanol to 10 μg/mL, then with water to prepare the standards at concentrations shown in the calibration graphs. The stock and standard solutions of CNO were prepared in acetonitrile/water (9:1 v/v) as described by Li et al., (2012). All stock and standard solutions were stored at −20°C until use. Each standard was prepared as 1) a neat standard and 2) as a standard in the plasma matrix, where the matrix is plasma from naïve untreated mice. The standard in the plasma matrix was prepared for LCMS in the same way as the biologic plasma sample as described in detail in the next section. A blank without any standard was prepared, and the background peak area in the blank was subtracted from the peak area of the standard in constructing the calibration graph. The internal standards, prepared at fixed concentrations of 3 ng/mL for 3-HC-d_3 and 8.55 ng/mL for CNO-d_3 in acetonitrile, were added to each calibration standard and the plasma sample.

Plasma Sample Preparation. The plasma sample was prepared for LCMS by a validated method (Kaisar et al., 2017). Briefly, 10 μL of each plasma sample was mixed with 80 μL of acetonitrile containing the internal standard, vortex mixed, and centrifuged at 9660g for 25 minutes at 4°C to precipitate plasma proteins. This treatment results in a ninefold dilution of the standard or the analyte and a 1.125-fold dilution of the internal standard. Seventy microliters of the clear supernatant were transferred to a precleaned and dried LCMS vial. The standard in the plasma matrix was prepared in the same way. Specifically, to prepare a 3.3 ng/mL 3-HC standard in the plasma matrix, we added 3 μL of 30 ng/mL 3-HC standard to 27 μL of plasma from naïve mice, followed by vortex mixing and the addition of 240 μL of acetonitrile containing 3.0 ng/mL of the internal standard 3-HC-d_3. Following vortex mixing and centrifugation at 9660g at 4°C for 25 minutes to precipitate plasma proteins, 210 μL of the clear supernatant was transferred to an LCMS vial for injection. The injection volume was 4 μL for 3-HC, 5-HC, and cotinine and 10 μL for CNO. In our previous study (Nguyen et al., 2020), we confirmed, by recovery studies, that plasma cotinine is well preserved during protein precipitation with acetonitrile. The quality control samples contained *trans* 3-HC, 3-HC-d_3, 5-HC, CNO, and CNO-d_3 at final concentrations of 16.67, 2.67, 16.67, 22.2, and 7.6 ng/mL, respectively (after the dilutions described above), and were acquired every 1.8 hours to monitor instrument stability.

Precision and Accuracy. Precision, defined as the closeness of measurements of the same concentration, was assessed in the present study by performing LCMS assays of the plasma 3-HC and 5-HC concentrations in nicotine-treated mice twice and examining the percentage difference between the first and the second assay. Accuracy, defined as the closeness between measured and true concentration, was assessed for the CNO standard in the plasma matrix by measuring (Peak area$_{test}$/Peak area$_{reference}$) × (100), where "test" refers to the addition of a known quantity of CNO to the matrix before the addition of acetonitrile (1:8 v/v) and centrifugation to precipitate plasma protein, and "reference" refers to the addition of the corresponding quantity of CNO after the acetonitrile treatment and removal of plasma protein. This was designed to test the recovery of CNO after the acetonitrile treatment.

Liver Microsome Preparation. Liver microsome was prepared from frozen liver tissues with BioVision microsome isolation kit according to the manufacturer's instruction. Briefly, the liver tissue, stored at −80°C, was thawed and gently homogenized (15–20 strokes) in Dounce homogenizer after adding the homogenizing buffer containing sucrose and protease inhibitor cocktail (1 mL/400 mg of tissue). The homogenate was centrifuged at 10,800g for 15 minutes to precipitate cell debris, and this procedure was repeated twice. In removing the supernatant containing the microsomes, care was taken to avoid aspirating the floating lipid layer. The supernatant was then centrifuged at 38,700g for 20 minutes in a Sorvall RC5C Plus centrifuge. This resulted in the separation of a pink, translucent microsomal pellet. All operations were performed at 4°C. The microsome pellet was suspended in the storage buffer and stored at −80°C until use.

Coumarin 7-Hydroxylase Activity. The activity was assayed as previously described (Aitio, 1978). The assay mixture contained 10 μM coumarin and 100 μM NADPH in phosphate buffer at pH 7.4. Each microsomal preparation was added at two different dilutions to ensure accuracy. The mixture (100 μL) was incubated at 37°C for 10 minutes, followed by the addition of 0.32 M trichloroacetic acid (100 μL) to terminate the reaction and the addition of 3.2 M glycine/NaOH buffer (100 μL) to quench residual NADPH (Aitio, 1978). After removal of denatured microsomal protein by centrifugation (9660g) at 4°C for 10 minutes, 7-hydroxycoumarin in the supernatant was assayed in duplicates by fluorometric detection at 360/460 nm (excitation/emission) in a Biotek Synergy II microplate reader (Winooski, VT) located at Lab Launch, Monrovia. The fluorescence in the assay mixture without incubation (control) was subtracted from the fluorescence in the incubated mixture, then converted to 7-hydroxycoumarin concentration by calibration with the standard. LCMS-grade water was used for the preparation of all reagents and the cleaning of vials and pipette tips to ensure low background fluorescence. Coumarin 7-hydroxylase activity was calculated from the pmol of 7-hydroxycoumarin formed per min per mg of microsomal protein. The reported activity is the mean of the activities determined at two different microsomal dilutions. Microsomal protein concentration was determined by Bradford assay.

Statistical Analyses. Data are expressed as the mean ± standard deviation. Data were analyzed using two-way ANOVA or unpaired two-tailed Student's t test, whichever appropriate, as indicated in each figure legend, using GraphPad Prism 9 (GraphPad Software Inc., San Diego, CA).

Results

Identification of 3-HC, 5-HC, and CNO. In experiments designed to identify 3-HC in the plasma samples of nicotine-injected mice, we used an estimated retention time of 1.86 ± 0.3 minutes for *trans* 3-HC, based on our preliminary results with neat *trans* 3-HC standard under our chromatographic conditions. To our surprise, we found two peaks, with retention times of 1.74 and 1.95 minutes, both with m/z of 193.0977, which corresponds to the $[M+H]^+$ parent ion of 3-hydroxy-cotinine. This suggested that the second peak represented an isomer of 3-HC with the same mass. A likely candidate was 5-HC (Fig. 1), which had been detected in vitro upon incubation of recombinant human CYP2A6 with hamster liver microsome and cotinine (Murphy et al., 1999). A subsequent LCMS experiment with authentic 5-HC identified the peak with the retention time of 1.75 minutes as 5-HC (Fig. 2C). The assignment was confirmed by spiking plasma samples from nicotine-injected mice with 5-HC, which resulted in the increased peak area of only the 1.75-minute peak (result not shown). The peak with the retention time of 1.95 minutes was assigned to *trans* 3-HC; this was confirmed by the retention time of *trans* 3-HC standard (Fig. 2A) and of *trans* 3-HC-d_3 (Fig. 2B). Note that the 3-HC chromatogram shows 5-HC peak too because this was prepared as a mixed standard containing both 3-HC and 5-HC.

CNO was examined separately from 3-HC and 5-HC due to its expected high polarity (Fig. 1). The retention time was 2.96 minutes for CNO and CNO d_3 (Fig. 2, D and E). Table 1 lists the retention times of 3-HC, 5-HC, and CNO when measured as standards in the plasma matrix and the m/z values of their parent $[M+H]^+$ ion and of their deuterated counterparts used as an internal standard.

Sensitivity and Calibration. In Fig. 2, A–E, the concentration of each standard prepared in the plasma matrix is shown for the respective LCMS chromatogram to demonstrate sensitivity. *Trans* 3-HC at the final concentration of 3.3 ng/mL showed a peak area of 54064 (Fig. 2A), and 5-HC at 1.1 ng/mL showed a peak area of 14547 (Fig. 2C). Thus, sensitivity is quite high for the standard of both metabolites. CNO at 2.2 ng/mL had a peak area of 282 (Fig. 2D), resulting in a lower but acceptable signal-to-noise ratio at this concentration. The much lower
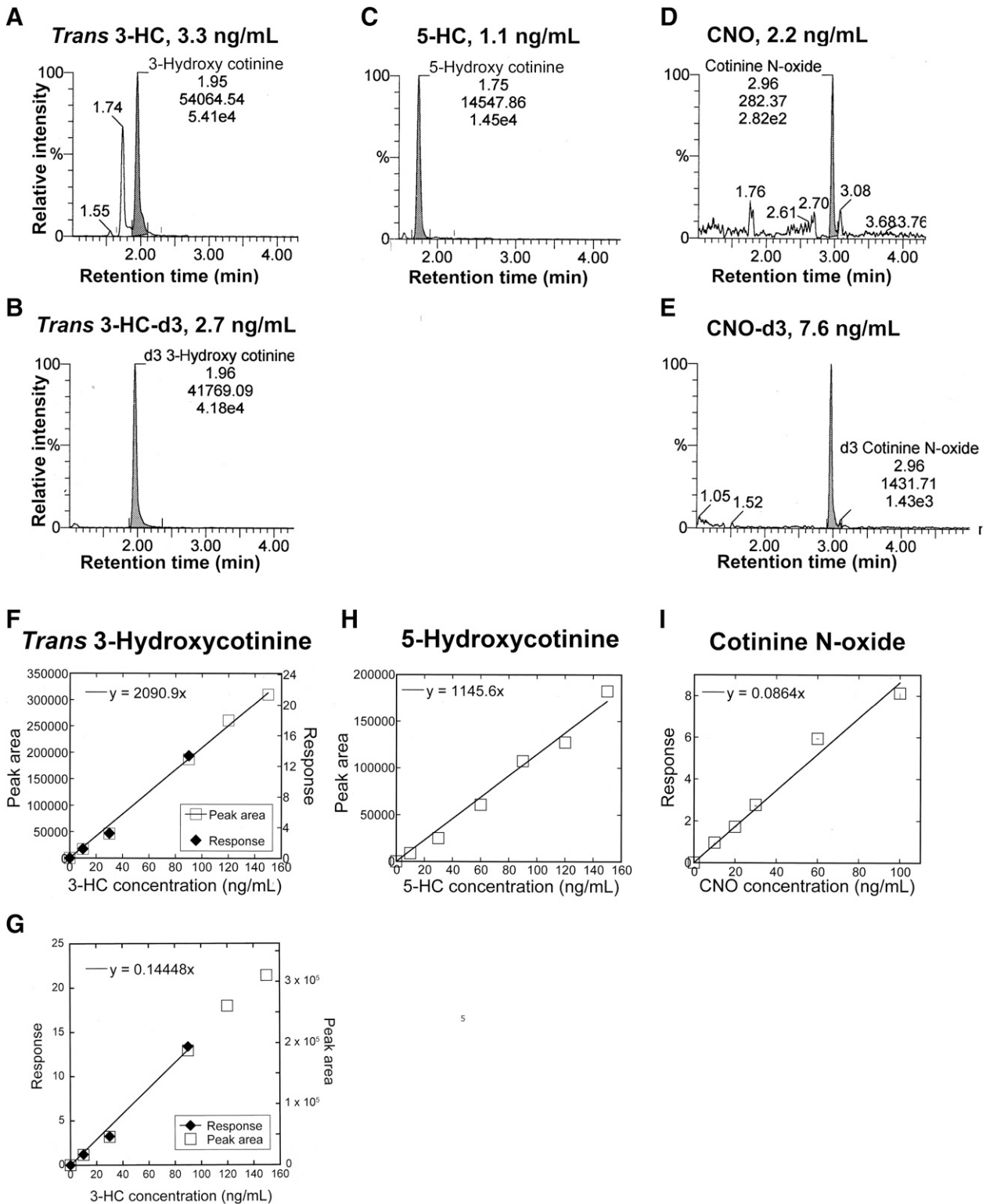
Fig. 2. LCMS chromatograms of *trans* 3-hydroxycotinine (A), *trans* 3-hydroxycotinine-d₃ (B), 5-hydroxycotinine (C), cotinine-N-oxide (D), and cotinine-N-oxide-d₃ (E) standards prepared in plasma matrix. The concentration of each metabolite in the standard is shown at the top, and the relevant peak is shaded. Note that *trans* 3-HC standard was acquired as a mixed standard with 5-HC, whereas 5-HC and CNO standards were acquired as single standards. The annotation shows the compound name, the retention time, the peak area, and the peak area in scientific notation. The vertical axis shows relative peak intensity, with the tallest peak as 100%. Calibration graphs of *trans* 3-HC (F and G), 5-HC (H), and CNO (I). Calibration was performed by measuring, at each standard concentration, either the peak area (as in 5-HC) or the response = peak area*IS conc./IS peak area, where IS is the deuterated internal standard (as in CNO) or both (3-HC). The slope of the equation shown in each graph was used to convert the peak area or response of the metabolite in plasma samples to metabolite concentration.

TABLE 1

The retention time and the m/z of the parent [M+H]$^+$ ion of each standard (prepared in plasma matrix) and its respective internal standard

Standard Compound	RT (min)	[M + H]$^+$ (m/z)
Cotinine	2.02	177.1062
Cotinine-d$_3$	2.02	180.1312
Trans 3-hydroxycotinine	1.94–1.95	193.0977
Trans 3-hydroxycotinine-d$_3$	1.96	196.1162
5-Hydroxycotinine	1.75	193.0977
Cotinine N-oxide	2.96	193.0977
Cotinine N-oxide d$_3$	2.96	196.1173

peak area for CNO compared with 3-HC and 5-HC is because CNO is a much more polar compound (Fig. 1), resulting in greater signal suppression.

For calibration of 3-HC, two standard graphs were prepared: 1) as peak area versus concentration and 2) as response = peak area*IS conc./IS peak area versus concentration, where the internal standard (IS) is the deuterated 3 HC-d$_3$. The former is shown in Fig. 2F, with the peak area on the left y-axis and the response on the right. The equation of the least-squares line was y = 2090.9x (Fig. 2F). For response, the equation obtained separately was y = 0.1445x (Fig. 2G). These equations were used to convert the observed peak area or response in each plasma sample to metabolite concentration.

The r^2 value, defined as (the square of the correlation coefficient) × 100, was 99.7 and 99.1 for the peak area and the response, respectively. This response was used when it was important to monitor instrument stability during long total run times required when the number of plasma samples was large. Note that the concentration shown in these calibration graphs is the concentration of each standard *before* the addition of acetonitrile to precipitate plasma protein. The reason is that the standard in the plasma matrix was prepared for LCMS assay in the same way as the biologic plasma (as described in detail in *Materials and Methods*). Consequently, it is appropriate to use the predilution concentration of the standard to quantify the metabolite in biologic plasma samples.

For 5-HC, no deuterated compound was available, so the calibration graph consisted of the peak area plotted against concentration (Fig. 2H; r^2 = 98.8). The equation was used to convert the peak area in each plasma sample to 5-HC concentration. Figure 2I shows the calibration graph of CNO as the response, with CNO-d$_3$ as an internal standard and as the mean of duplicate LCMS assays. The calibration graph of CNO as response shows good linearity (r^2 = 98.4), permitting its quantification in the plasma samples. We used response for calibration of CNO because signal suppression occurs for both CNO and CNO-d$_3$, and as a result, differences in the slopes of the calibration graph among standards of different polarity are much smaller when expressed as the response instead of as peak area.

For direct MS detection, detector saturation can occur at high concentration. Detector saturation was examined at each concentration of the standard and was found not to occur for standards prepared in the plasma matrix at the concentrations shown in the calibration graphs.

For e-cig–treated mice only, we quantified plasma cotinine too by the MS method, as shown in a representative LCMS chromatogram and cotinine calibration graph provided in Supplemental Fig. 1. The reason is that the MS method provided a clean background for the parent ion of cotinine with m/z 177.1062 (Table 1), whereas when cotinine was assayed by the tandem MS method through its product ion with m/z of 98.06, there was a high background. This suggests that the e-cig used in our study contains a compound(s) that coelutes with the product ion of cotinine with m/z of 98.06. By contrast, in the plasma of mice given

nicotine injection, cotinine assayed by the tandem MS method through the product ion (m/z 98.06) had a clean background, as reported in our previous study (Nguyen et al., 2020). Accordingly, for nicotine-injected mice, the plasma cotinine levels reported previously are used for comparison with those of 3-HC, 5-HC, and CNO.

3-HC, 5-HC, and CNO after Nicotine Injection. Figure 3A shows representative LCMS chromatograms of the plasma sample collected 15 minutes after nicotine injection (1 mg/kg) in a C57BL/6 female mouse. The quantified metabolite is shown by the shaded peak and is annotated with its retention time and the peak area for 3-HC (top panel) and 5-HC (middle panel). For CNO (bottom panel), the CNO peak is plotted with 100% intensity in the inset and labeled with the compound name, the retention time, and the peak area. The 3-HC, 5-HC, and CNO concentrations in this plasma sample, quantified by calibration with standards, were 163.8, 157.9, and 70.7 ng/mL, respectively. Plasma nicotine and cotinine levels reported previously (Nguyen et al., 2020) using the same plasma as the current study were 471.0 and 670.5 ng/mL, respectively.

Although the peaks of 5-HC and CNO are sharp, the 3-HC peak at 1.94 minutes shows a shoulder on the right at 2.02 minutes. For *trans*
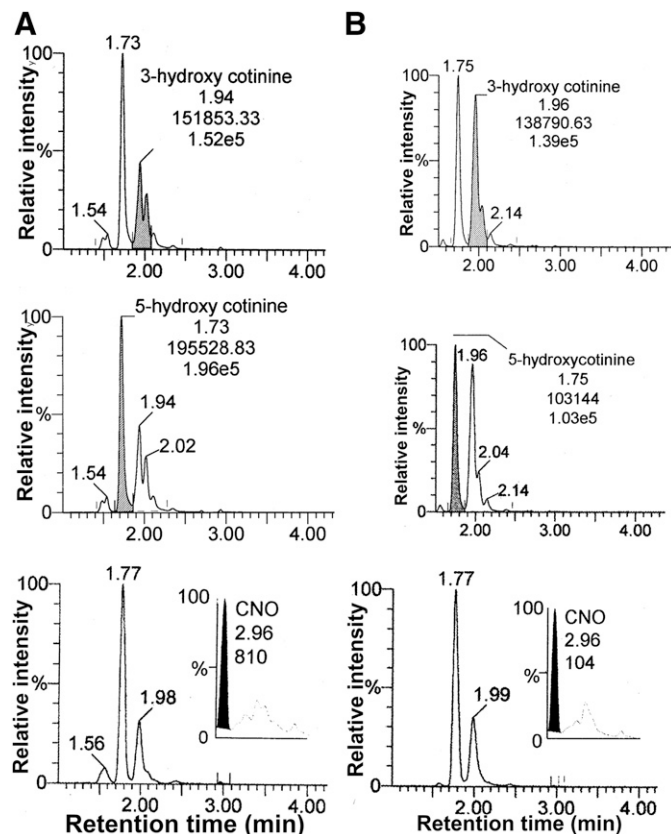

Fig. 3. (A) Representative LCMS chromatograms of the plasma sample collected 15 minutes after nicotine injection (1 mg/kg) in a C57BL/6 female mouse, showing 3-HC (shaded peak, top panel) and 5-HC peak (shaded peak middle panel). The annotations show the compound name, the retention time, the peak area, and the peak area in scientific notation. For CNO (bottom panel), the CNO peak is plotted with 100% intensity in the inset with annotation of the compound name, the retention time, and the peak area. (B) Representative LCMS chromatograms of the plasma samples collected 5 to 6 minutes after a male C57BL6 mouse was exposed to an e-cig containing 2.4% nicotine for 4 hours. 3-HC (shaded peak, top panel) and 5-HC peak (shaded peak middle panel) are shown. For CNO (bottom panel), the CNO peak is plotted with 100% intensity in the inset. Annotations as explained in (A). Note that in the top and middle panels, the retention time starts at 1.5 minutes, whereas in the bottom panel, it starts at 1.0 minutes because the latter was acquired on a separate day. The retention time scales are aligned.

3-HC standard in the plasma matrix (Fig. 2A), the main peak (RT 1.95 minutes) has a small shoulder at 2.03 minutes. In the plasma samples, the shoulder is larger. The integrated area over the 1.94–2.05-minute region, including the shoulder at 2.02 minutes, was assigned to 3-HC (for explanation, see *Discussion*).

3-HC, 5-HC, and CNO after E-Cig Treatment. Figure 3B shows representative LCMS chromatograms of the plasma sample collected 5 to 6 minutes after a C57BL/6 male mouse was exposed to an e-cig containing 2.4% nicotine for 4 hours. 3-HC eluting at 1.96 minutes had a peak area of 138790 (top panel), 5-HC at 1.75 minutes had peak area of 103144 (middle panel), and CNO at 2.96 minutes had a peak area of 104 (bottom), respectively. Corresponding plasma concentrations of 3-HC, 5-HC, and CNO were 119.4, 75.4, and 9.5 ng/mL, respectively. The result shows that in this mouse with a plasma nicotine level of 40.2 ng/mL that simulates the level in human smokers and a plasma cotinine level of 138.3 ng/mL, these three oxidation products of cotinine formed by CYP2A5 are clearly detectable in the plasma collected at 5 to 6 minutes after the end of the 4-hour exposure time. The LCMS chromatograms of cotinine and nicotine in this e-cig–treated mouse are provided in Supplemental Figs. 1 and 2, respectively.

Male-Female Differences in Cotinine Oxidation Products. Figure 4A shows the plasma concentrations of 3-HC, 5-HC, and CNO, as the mean ± S.D. of $N = 5$ to 6, in male and female mice given nicotine injection (1 mg/kg) 15 minutes before blood collection. At 15 minutes postinjection, plasma nicotine and cotinine are in equilibrium (Siu and Tyndale, 2007). The concentrations of the nicotine-induced oxidation products of cotinine are significantly higher than in the control for each metabolite. We assessed the precision and accuracy of these metabolite concentration measurements. As a measure of precision, we examined the percentage difference between the first and second LCMS assay of plasma metabolites in nicotine-treated mice. As shown in Supplemental Table 1, for 3-HC, which was calibrated by the response, the

concentration determined in the first assay differed from that in the second assay by less than 5.2% in all treatment groups (male and female). For 5-HC, calibrated by the peak area, the difference was 4.6%–19.4%, depending on the treatment. Note that, by the Food and Drug Administration requirements for clinical studies, acceptable precision for the relative standard deviations of the lower limit of quantification standards is 20%. In the present study, plasma 5-HC was quantified from the peak area of the first assay for nicotine-injected mice and the mean peak area of the two assays for the e-cig–treated mice. Accuracy, a measure of the closeness of the measured and true concentration, was assessed by recovery as described in *Materials and Methods*. Recovery was 95% for the CNO standard in the plasma matrix at 3.3 ng/mL. For cotinine, the recovery was 96.3 ± 4.7% as determined previously in our laboratory (Nguyen et al., 2020). These results show that the metabolite concentration measurements shown in Fig. 4 have acceptable precision and accuracy.

As shown in Fig. 4A, the plasma concentration of 3-HC is higher in female than in male mice ($P < 0.05$). It is important to note that the plasma concentration of 5-HC, not detected previously in vivo in mouse plasma, is higher than that of 3-HC in the males and as high as that of 3-HC in the females. The plasma concentration of CNO, also detected for the first time in mouse plasma, is lower but quantitively significant. The results clearly show that 5-HC and CNO must be considered in examining the cotinine oxidation pathway in vivo. Figure 4B compares the male-female difference in the plasma concentrations of cotinine (left), of cotinine plus 3-HC plus 5-HC plus CNO (middle), and of 3-HC plus 5-HC plus CNO (right) in mice given 1 mg/kg nicotine injection 15 minutes before blood sampling. In the figure on the left, taken from our previous publication (Nguyen et al., 2020), the male-female difference in plasma cotinine (COT) concentration did not reach a significant difference ($P = 0.056$). When plasma (COT plus 3-HC plus 5-HC plus CNO) concentration is examined (middle panel), the female
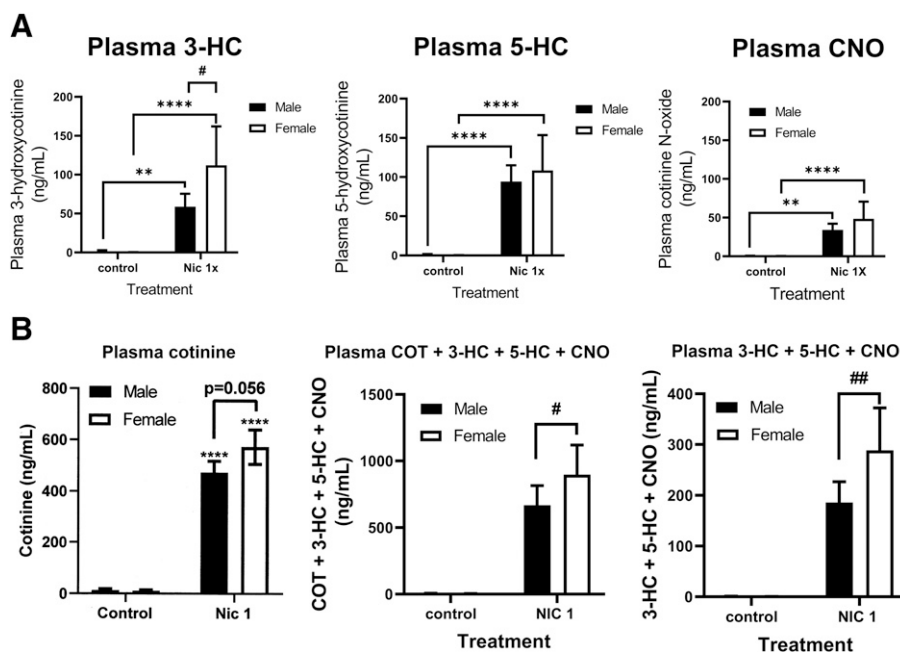
Fig. 4. (A) Plasma concentrations of 3-HC, 5-HC, and CNO measured at 15 minutes after subcutaneous injection of nicotine (1 mg/kg)(Nic 1x) in male and female WT C57BL/6 mice compared with control. The data are mean ± S.D. ($N = 5$ to 6 for each sex and treatment). For 3-HC, two-way ANOVA with Tukey's multiple comparisons test was used to analyze male-female difference (#$P < 0.05$) and treated versus control (**$P < 0.01$; ****$P < 0.0001$). For 5-HC and CNO, two-way ANOVAs with Tukey's and Sidek's multiple comparisons test, respectively, were used to analyze the treated versus control difference (**$P < 0.01$; ****$P < 0.0001$). (B) The male-female difference in the plasma concentrations of cotinine (left), of COT plus 3-HC plus 5-HC plus CNO (middle), and of 3-HC plus 5-HC plus CNO (right) in mice given 1 mg/kg nicotine injection 15 minutes before blood sampling. The data are mean ± S.D. for $N = 5$ to 6 for each treatment and sex. Male-female differences by two-way ANOVA with Sidek's multiple comparisons test (#$P < 0.05$; ##$P < 0.01$).

TABLE 2

Relative percentages of 3-HC, 5-HC, and CNO in the combined plasma (3-HC plus 5-HC plus CNO) concentration in male and female mice after nicotine injection

Treatment	3-HC		5-HC		CNO	
	Male	Female	Male	Female	Male	Female
Nic 1x	31.4	41.6	50.4	40.4	18.2	18.0
Sal 6x Nic 1x	34.6	41.2	47.1	42.8	18.3	16.0
Nic 7x	40.1	44.6	41.9	38.2	18.0	17.2

level is significantly higher than the male level, with $P = 0.036$ (# in the figure). For plasma (3-HC plus 5-HC plus CNO) concentration (right panel), the male-female difference is even greater, with $P = 0.008$ (##). The result highlights the importance of examining all three oxidation products of cotinine in studying the male-female difference in nicotine metabolism and disposition. Table 2 lists the relative percentages of 3-HC, 5-HC, and CNO in the combined plasma (3-HC plus 5-HC plus CNO) concentration in the nicotine-injected male and female mice.

The Effect of Repeated Nicotine Injection. Figure 5A shows the plasma 3-HC (left), 5-HC (middle), and CNO (right) concentrations in male and female mice that were pretreated with saline injection (Sal) for 6 days, followed by 1 mg/kg nicotine injection (Nic) on day 7 (Sal 6x, Nic 1x), or given 1 mg/kg nicotine injection per day for 7 days (Nic 7x). After repeated nicotine injections for 7 days, female mice show

significantly higher levels of 3-HC than male ($P = 0.004$), and also of 5-HC ($P = 0.021$) and CNO ($P = 0.0369$). By contrast, after saline pretreatment, followed by one nicotine injection, the male-female difference does not reach a significant difference. The result shows that repeated nicotine treatment enhances the formation of the three oxidation products of cotinine in females to a greater extent than in males.

Our previous study (Nguyen et al., 2020) compared plasma cotinine concentrations under those two treatments and found that plasma cotinine levels were significantly higher in females than in males under both conditions (Fig. 5B, left panel). The right panel compares the level of plasma (3-HC plus 5-HC plus CNO) concentration under these two treatments in male and female mice. After pretreatment with saline, there is no significant male-female difference. However, after repeated nicotine administration, female mice show a significantly higher level of (3-HC plus 5-HC plus CNO) than males ($P = 0.0068$). The higher (3-HC plus 5-HC plus CNO) level in females relative to males after repeated nicotine treatment can be due to 1) the higher cotinine level in the female after repeated nicotine level (left panel) and/or 2) higher CYP2A5 activity in females than in males.

Coumarin 7-Hydroxylase Activity in Male and Female Mice. To examine the latter possibility, we investigated, as the first step, coumarin 7-hydroxylase activity, as a specific measure of CYP2A5 activity (Raunio et al., 2020), in the liver microsomes of untreated male and female wild-type (WT) C57BL/6 mice. Figure 6 shows coumarin 7-hydroxylase activity in untreated male and female WT C57BL/6 mice. The data are shown in a box plot with the individual values for $N = 8$.
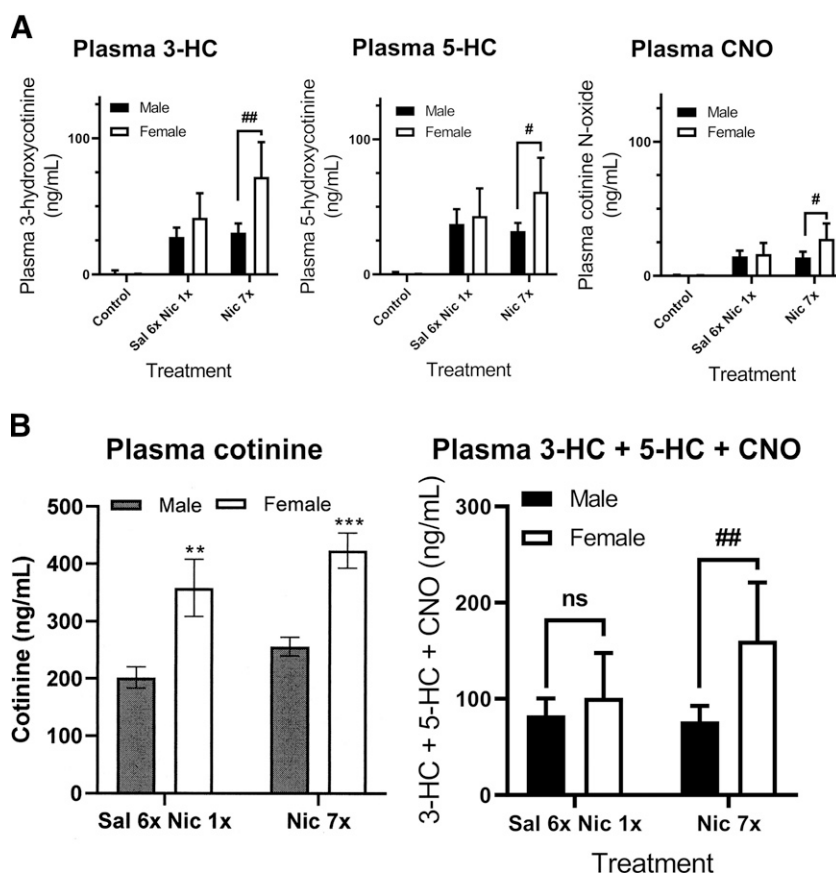

Fig. 5. (A) Plasma concentrations of 3-HC, 5-HC, and CNO measured at 15 minutes after nicotine (1 mg/kg) injection on day 7 following pretreatment with saline or nicotine (1 mg/kg) for 6 consecutive days in male and female WT C57BL/6 mice. The data are mean ± S.D. of $N = 4$–6 for each treatment and sex. Male-female difference by two-tailed t test (#$P < 0.05$; ##$P < 0.01$). (B) Plasma concentrations of 3-HC plus 5-HC plus CNO (right panel) in the same mice. Plasma (3-HC plus 5HC plus CNO) concentration is higher in female than in male mice (## $P < 0.001$ by two-way ANOVA with Sidak's multiple comparisons test) after repeated treatment with nicotine (Nic 7x), but no difference is seen after saline treatment (Sal 6x Nic 1x). The left panel shows plasma cotinine concentration in the same mice reported in our previous publication.
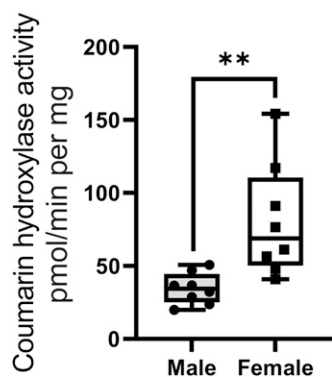
Fig. 6. Coumarin 7-hydroxylase activity, as a specific marker of CYP2A5 activity, in the liver microsomes prepared from untreated male and female mice. The data are shown in a box plot with the individual values for $N = 8$. The line indicates the median activity, and whiskers indicate the minimum and the maximum activities. The male-female difference was examined by Mann-Whitney U test (**$P = 0.011$).

The line indicates the median activity, and whiskers indicate the minimum and the maximum activities. The median activity for females was significantly higher than that of males (**$P = 0.011$; Mann-Whitney U test). The result shows that CYP2A5 activity is significantly higher in female mice than in males, with the activities in the female displaying greater interanimal variability than in the male.

Cotinine Oxidation Products in E-Cig–Treated Male Mice. Figure 7 shows nicotine, cotinine, 3-HC, 5-HC, and CNO concentrations in the plasma of male mice collected at the end of the 4-hour exposure to an e-cig containing 2.4% nicotine ("e-cig acute" in the fig) or 0% nicotine (control). The data are mean ± S.D. ($N = 3$ for each group).

The measurements of plasma nicotine by LC-MS/MS and of cotinine by direct MS in the e-cig–treated mice are described in Supplemental Figs. 2 and 1, respectively. The metabolite level after exposure to an e-cig containing 2.4% nicotine is significantly higher than in the control, with **$P < 0.01$ or ***$P < 0.001$. Although the number of animals is small in this pilot study, the result clearly shows that at the plasma nicotine level of 55.7 ± 16.0 ng/mL, simulating that of human smokers, cotinine (151.5 ± 47.3 ng/mL) and 3-HC (157.2 ± 51.9 ng/mL) are formed in significant quantities. Furthermore, 5-HC (91.9 ± 16.9 ng/mL) and CNO (12.5 ± 3.1 ng/mL), not previously detected in mouse plasma, are also formed in significant or measurable amounts. It is worth mentioning that livers were collected from these e-cig–treated mice (though not from nicotine-injected mice), and coumarin 7-hydroxylase activity was measured in microsomes prepared from those livers. The mean
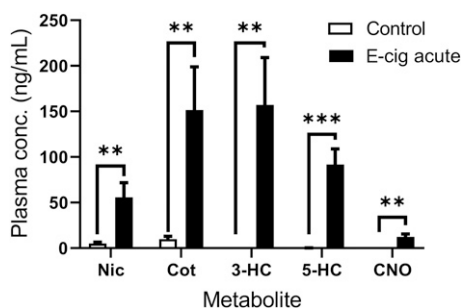

Fig. 7. The concentrations of nicotine, cotinine, 3-HC, 5-HC, and CNO in the plasma of male mice, collected 5 to 6 minutes after exposure to an e-cig containing 2.4% nicotine (e-cig acute) or 0% nicotine (control) for 4 hours. The data are mean ± S.D. ($N = 3$ for each group). Each metabolite level in the e-cig acute group was compared with the control by two-tailed t test (**$P < 0.01$; ***$P < 0.001$).

coumarin 7-hydroxylase activity in the e-cig–treated male mice was 21.6 ± 6.0 pmol/mg per minute. This is within the range of activity found in untreated male mice (Fig. 6). Taken together, our results show that, at the plasma nicotine level mimicking that of human smokers, significant quantities of its CYP2A5-catalyzed oxidation products, viz cotinine, 3-HC, 5-HC, and CNO are formed even in male mice with relatively low CYP2A5 activity.

Discussion

We show for the first time that 5-HC and CNO are detectable in the mouse plasma after nicotine administration in vivo (Fig. 3). Previous studies had identified 5-HC and CNO in vitro upon incubation of 1) recombinant human CYP2A6 with hamster liver microsome and cotinine (Murphy et al., 1999) and 2) primary mouse hepatocyte culture with ^{14}C-cotinine (Foth et al., 1992), respectively. CNO was quantified in the plasma of rats (Li et al., 2012), in which oxidation of cotinine to CNO is catalyzed by CYP2B1, (Hammond et al., 1991, Nakayama et al., 1993), an enzyme that shows less similarity to human CYP2A6 than mouse CYP2A5. Our study shows that the plasma concentration of 5-HC is as high as that of 3-HC in nicotine-injected mice (Figs. 4A and 5A); the concentration of CNO, although lower, is quantitatively significant. As shown in Table 2, the relative percentages of 3-HC and 5-HC are similar, whereas the relative percentage of CNO is about one-half of that of the other two. The result shows that it is important to consider 5-HC, in addition to 3-HC, and to a lesser extent CNO, in examining the metabolism and disposition of cotinine in vivo.

For 3-HC, the shoulder on its peak (Fig. 3A) requires an explanation. It is unlikely to be due to the detection method for *trans* 3-HC because this shoulder is more pronounced in the plasma samples of nicotine-treated mice than in the *trans* 3-HC or *trans* 3-HC-d_3 standard (Fig. 2, A and B). Thus, it is possible that these plasma samples contain another metabolite with the same parent ion of m/z 193.0977 as *trans* 3-HC but with a retention time that partially overlaps that of *trans* 3-HC. One possibility is *cis* 3-HC. Voncken et al., (1990) reported that 11.8% of 3-HC excreted in hamster urine is the *cis* isomer, whereas it is predominantly *trans* 3-HC in human urine (Hukkanen et al., 2005). Because our major finding in the present work is the identification of 5-HC, which provides a sharp, well resolved peak, we did not pursue further the possible identity of the shoulder peak on 3-HC in these plasma samples.

Plasma 5-HC and CNO were quantified by directly detecting the parent ion (M+H)$^+$ with m/z of 193.0977. The high sensitivity provided by direct MS is useful for quantifying low-concentration metabolites with a limited sample volume, as in mouse plasma. Our method permitted quantification of these metabolites in 10 μL of plasma sample after it was diluted ninefold with acetonitrile containing IS, which is a simple and effective procedure for plasma protein precipitation. The injection volume was 4 μL, except for CNO, where 10 μL was injected. In nicotine-injected rats, plasma CNO and 3-HC were detected by LC-MS/MS after metabolite purification by solid-phase extraction (Li et al., 2012).

The reason why 5-HC was not detected previously may not have been just a question of the sensitivity of the detection method but because previous researchers did not screen their samples for 5-HC. 3-HC and 5-HC share the same product ions with m/z 134 and 80. For 3-HC, the m/z 134 ion has been used as the identifier and the m/z 80 ion as the quantifier. Fortunately, 5-HC has unique product ions with m/z 162 and 106 that can be detected by optimizing the collision energy, as reported by (Murphy et al., 1999). This provides a way to monitor 5-HC by LC-MS/MS.

In nicotine-injected mice, the male-female difference in plasma cotinine did not reach statistical significance (Fig. 4B, left panel; $P = 0.056$). However, when we examined the combined plasma concentration of

cotinine plus 3-HC plus 5-HC plus CNO (middle panel), the concentration was higher in female than male mice ($P = 0.036$). For plasma concentration of 3-HC plus 5-HC plus CNO (right panel), the difference was even greater ($P = 0.008$). A likely explanation is that although the metabolism of nicotine to cotinine is a two-step reaction requiring microsomal CYP2A5 and cytosolic aldehyde oxidase, the oxidation of cotinine to 3-HC, 5-HC, and CNO is catalyzed by a single enzyme, CYP2A5 (Fig. 1). For hepatic aldehyde oxidase in adult C57BL/6 mice, the activity measured in the cytosol of liver homogenate was 2 to 3 times higher in the male than in the female with the level of this enzyme regulated by sex hormones (Huff and Chaykin, 1967). Hence, sexual dimorphism of aldehyde oxidase appears to work opposite to that of CYP2A5. These considerations strongly suggest that oxidation of cotinine to 3-HC, 5-HC, and CNO catalyzed by CYP2A5 alone reflects better the male-female difference in CYP2A5 activity than the two-step oxidation of nicotine to cotinine.

This male-female difference was also found in mice given the same nicotine dose (1 mg/kg) for 7 days compared with their saline-treated controls, i.e., those that received saline for 6 days and then nicotine on day 7 (Fig. 5A). Although no male-female difference was seen after pretreatment with saline in any of the metabolites, repeated nicotine treatment resulted in higher 3-HC in females than males ($P = .004$) and higher 5-HC and CNO ($P = 0.021$ and 0.0369, respectively) in female than in male mice. Consequently, the combined plasma concentration of 3-HC plus 5-HC plus CNO was higher in females than in males after repeated nicotine treatment (Nic 7x) ($P = 0.0068$), whereas no significant difference was seen after saline pretreatment (Fig. 5B, right panel). These results can be explained by a higher concentration of the substrate cotinine (Fig. 5B, left panel) and/or higher CYP2A5 activity in the female mice.

Coumarin 7-hydroxylase activity, a specific marker of CYP2A5 activity, was also higher in liver microsomes of females than males by Mann-Whitney U test (Fig. 6). The activity in the males showed little variability. However, the activity in the female mice showed high interanimal variability. A previous study (van Iersel et al., 1994) reported that, in naïve C57BL/6 mice, coumarin 7-hydroxylase activity was not significantly different between males and females when the mean of $N = 4$ was compared. Subsequent studies in nicotine self-administrating C57B1/6 mice showed a higher CYP2A5/CYP2A4 protein density in females than male mice (Siu et al., 2006). Recently, the vitro rate of CYP2A5-catalyzed oxidation of nicotine to nicotine-iminium ion (Fig. 1) was shown to exhibit a higher median, as well as a larger interanimal variability, in female than in male nicotine-injected C57BL/6 mice (Bloom et al., 2019). Our present finding that CYP2A5 activity is higher in female than in male mice ($N = 8$ for each sex) is in accord with these recent reports. These considerations strongly suggest that the higher (3-HC plus 5-HC plus CNO) concentration in female than in male mice found after repeated nicotine injection (Fig. 5) can most reasonably be attributed to higher CYP2A5 activity in females. Whether repeated nicotine treatment upregulates CYP2A5 and whether the mechanism of regulation differs between male and female mice are intriguing questions for future investigation.

In e-cig–treated male mice with plasma nicotine levels resembling those of human smokers and low microsomal CYP2A5 activity, plasma cotinine, 3-HC, and 5-HC were abundant, whereas CNO was low but measurable at the end of the 4-hour exposure time (Fig. 7). It is likely that this 4-hour exposure period allowed time for extensive oxidation of cotinine to take place, despite its lower concentration compared with that in nicotine-injected mice. Cotinine has $t_{1/2}$ of ~38 minutes in the plasma of C57BL/6 mice (Siu and Tyndale, 2007; Zhou et al., 2010). A possible reason for the lower CNO concentration (12.5 ± 3.0 ng/mL) in e-cig–treated male mice compared with that in nicotine-treated mice

(34.0 ± 8.0 ng/mL) is the threefold lower concentration of the substrate cotinine in the former. However, further studies are needed to fully understand the pharmacokinetics of the three oxidation reactions of cotinine.

The identification of 5-HC in the plasma of nicotine-treated mice raises some interesting questions. The first is its route of disposition. Oxidation of cotinine to the more polar and water-soluble 3-HC and CNO facilitates renal excretion. 5-HC is likely to resemble 3-HC in these respects. Previous studies have shown that after administration of nicotine (10 mg/kg, p.o. (per os, by mouth)) to CD2F1 mice, urine collected for 24 hours contained 3-HC as the major product (77% of the total amount of nicotine-related material), followed by CNO (16%), whereas cotinine represented 3% to 4% (Raunio et al., 2008). In their work, 3-HC and CNO were quantified by LC-MS/MS through their product ions. In the urine of rats treated with ^{14}C-cotinine, 5-HC was isolated (Morselli et al., 1967). However, subsequent studies showed that hepatic oxidation of nicotine to cotinine in the rat is catalyzed by CYP2B1 (Hammond et al., 1991; Nakayama et al., 1993), an enzyme that shows little resemblance to mouse CYP2A5. In human smokers, trans 3-HC and its glucuronide accounted for more than 45% and CNO 2%–5% in the molar percentage of total recovered nicotine and metabolites in the 24-hour urine (Benowitz et al., 1994). The presence of 5′-HC in the urine of human smokers is controversial (Introduction). Interestingly, the approximately equal rates of 3′- and 5′-cotinine hydroxylation by human P4502A6 upon incubation with hamster liver microsomes and cotinine in vitro (Murphy et al., 1999) are in accord with our present finding that approximately equal quantities of plasma 3-HC and 5-HC are formed by CYP2A5 in vivo in nicotine-treated mice. Thus, it would be interesting to examine whether LCMS can detect urinary excretion of 5-HC in nicotine-treated mice.

As reviewed by (Hukkanen et al., 2005), in humans, nicotine and cotinine undergo N-glucuronidation and 3-hydroxycotinine undergoes O-glucuronidation, but in mice, nicotine and cotinine glucuronides have not been detected. It remains to be determined whether the enzyme UDP-glucuronosyltransferase that catalyzes N-glucuronidation of nicotine and cotinine in humans also catalyzes O-glucuronidation of 3-HC. In humans, 5-HC too may form glucuronides—a possible reason that 5-HC has eluded detection, although glucuronidation at its hydroxyl group may present more steric hindrance than in 3-HC. Interestingly, some investigators (Benowitz and Jacob, 2000) reported that the excretion of 3-hydroxycotinine-O-glucuronide in human urine is induced by smoking. Thus, screening for 5-HC and its possible glucuronides in human urine may be useful in future smoking cessation studies.

The second question is the tissue of origin of plasma 5-HC. Although hepatic CYP2A5 is considered the primary site of nicotine metabolism, coumarin 7-hydroxylase activity was reported to be as high in the kidney as in the liver in C57BL/6 male mice (Salonpaa et al., 1992). Coumarin 7-hydroxylase activity of 10 pmol/min per mg in the kidney of male C57 mice has been reported (Seubert et al., 2002). These considerations raise the intriguing possibility that plasma cotinine undergoes tubular reabsorption in the kidney and is oxidized to 5-HC for renal excretion.

In conclusion, we have shown that two oxidation products of cotinine, 5-HC and CNO, can be measured and are quantitatively important, in addition to the previously reported trans 3-HC, in the plasma of mice treated with nicotine or exposed to e-cigarettes containing 2.4% nicotine when the plasma nicotine concentration mimics that of human smokers. When the plasma concentrations of all three oxidation products of cotinine were taken into account, the combined concentration was significantly higher in female than in male mice after nicotine injection, whereas for cotinine alone, the difference did not reach statistical significance. Coumarin 7-hydroxylase activity, a specific marker of CYP2A5, was higher in female than in male C57/BL6 mice. The results show

that, in future studies, it is important to take 5-HC and CNO into account in examining 1) nicotine metabolism and disposition in vivo and 2) sexual dimorphism of CYP2A5 activity. Our results also raise intriguing questions about the tissue of origin of 5-HC and its route of elimination, which may be addressed by use of the sensitive direct MS method presented here or by screening for 5-HC through its unique product ions by LC-MS/MS. Finally, whether these metabolites contribute to the behavioral and molecular changes induced by nicotine also remains to be addressed in the future.

Authorship Contributions

Participated in research design: Lutfy, Kanamori, Ahmad.
Conducted experiments: Kanamori, Ahmad, Lutfy, Shin, Hamid.
Performed data analysis: Kanamori.
Wrote or contributed to the writing of the manuscript: Kanamori, Lutfy.

References

Abu-Bakar A, Hakkola J, Juvonen R, Rahnasto-Rilla M, Raunio H, and Lang MA (2013) Function and regulation of the Cyp2a5/CYP2A6 genes in response to toxic insults in the liver. *Curr Drug Metab* 14:137–150.
Aitio A (1978) A simple and sensitive assay of 7-ethoxycoumarin deethylation. *Anal Biochem* 85:488–491.
Benowitz NL and Jacob 3rd P (2000) Effects of cigarette smoking and carbon monoxide on nicotine and cotinine metabolism. *Clin Pharmacol Ther* 67:653–659.
Benowitz NL, Jacob 3rd P, Fong I, and Gupta S (1994) Nicotine metabolic profile in man: comparison of cigarette smoking and transdermal nicotine. *J Pharmacol Exp Ther* 268:296–303.
Bloom AJ, Upadhyaya P, and Kharasch ED (2019) Strain-specific altered nicotine metabolism in 3,3′-diindolylmethane (DIM) exposed mice. *Biopharm Drug Dispos* 40:188–194.
Cashman JR, Park SB, Yang ZC, Wrighton SA, Jacob 3rd P, and Benowitz NL (1992) Metabolism of nicotine by human liver microsomes: stereoselective formation of trans-nicotine N′-oxide. *Chem Res Toxicol* 5:639–646.
Foth H, Aubrecht J, Höhne M, Walther UI, and Kahl GF (1992) Increased cotinine elimination and cotinine-N-oxide formation by phenobarbital induction in rat and mouse. *Clin Investig* 70:175–181.
Hammond DK, Bjercke RJ, Langone JJ, and Strobel HW (1991) Metabolism of nicotine by rat liver cytochromes P-450. Assessment utilizing monoclonal antibodies to nicotine and cotinine. *Drug Metab Dispos* 19:804–808.
Huff SD and Chaykin S (1967) Genetic and androgenic control of N1-methylnicotinamide oxidase activity in mice. *J Biol Chem* 242:1265–1270.
Hukkanen J, Jacob 3rd P, and Benowitz NL (2005) Metabolism and disposition kinetics of nicotine. *Pharmacol Rev* 57:79–115.
Kaisar MA, Kallem RR, Sajja RK, Sifat AE, and Cucullo L (2017) A convenient UHPLC-MS/MS method for routine monitoring of plasma and brain levels of nicotine and cotinine as

a tool to validate newly developed preclinical smoking model in mouse. *BMC Neurosci* 18:71.
Li P, Beck WD, Callahan PM, Terry Jr AV, and Bartlett MG (2012) Quantitation of cotinine and its metabolites in rat plasma and brain tissue by hydrophilic interaction chromatography tandem mass spectrometry (HILIC-MS/MS). *J Chromatogr B Analyt Technol Biomed Life Sci* 907:117–125.
Messina ES, Tyndale RF, and Sellers EM (1997) A major role for CYP2A6 in nicotine C-oxidation by human liver microsomes. *J Pharmacol Exp Ther* 282:1608–1614.
Morselli PL, Ong HH, Bowman ER, and McKennis Jr H (1967) Metabolism of (plus or minus)-cotinine-2-14C in the rat. *J Med Chem* 10:1033–1036.
Murphy SE (2021) Biochemistry of nicotine metabolism and its relevance to lung cancer. *J Biol Chem* 296:100722.
Murphy SE, Johnson LM, and Pullo DA (1999) Characterization of multiple products of cytochrome P450 2A6-catalyzed cotinine metabolism. *Chem Res Toxicol* 12:639–645.
Murphy SE, Raulinaitis V, and Brown KM (2005) Nicotine 5′-oxidation and methyl oxidation by P450 2A enzymes. *Drug Metab Dispos* 33:1166–1173.
Nakajima M, Yamamoto T, Nunoya K, Yokoi T, Nagashima K, Inoue K, Funae Y, Shimada N, Kamataki T, and Kuroiwa Y (1996) Role of human cytochrome P4502A6 in C-oxidation of nicotine. *Drug Metab Dispos* 24:1212–1217.
Nakayama H, Okuda H, Nakashima T, Imaoka S, and Funae Y (1993) Nicotine metabolism by rat hepatic cytochrome P450s. *Biochem Pharmacol* 45:2554–2556.
Nega S, Marquez P, Hamid A, Ahmad SM, and Lutfy K (2020) The role of pituitary adenylyl cyclase activating polypeptide in affective signs of nicotine withdrawal. *J Neurosci Res* 98:1549–1560.
Neurath GB (1994) Aspects of the oxidative metabolism of nicotine. *Clin Investig* 72:190–195.
Nguyen K, Kanamori K, Shin CS, Hamid A, and Lutfy K (2020) The Impact of Sex on Changes in Plasma Corticosterone and Cotinine Levels Induced by Nicotine in C57BL/6J Mice. *Brain Sci* 10:705–719.
Raunio H, Pentikäinen O, and Juvonen RO (2020) Coumarin-Based Profluorescent and Fluorescent Substrates for Determining Xenobiotic-Metabolizing Enzyme Activities In Vitro. *Int J Mol Sci* 21:4708–4725.
Raunio H, Pokela N, Puhakainen K, Rahnasto M, Mauriala T, Auriola S, and Juvonen RO (2008) Nicotine metabolism and urinary elimination in mouse: in vitro and in vivo. *Xenobiotica* 38:34–47.
Salonpää P, Iscan M, Pasanen M, Arvela P, Pelkonen O, and Raunio H (1992) Cerium-induced strain-dependent increase in Cyp2a-4/5 (cytochrome P4502a-4/5) expression in the liver and kidneys of inbred mice. *Biochem Pharmacol* 44:1269–1274.
Seubert JM, Webb CD, and Bend JR (2002) Acute sodium arsenite treatment induces Cyp2a5 but not Cyp1a1 in the C57Bl/6 mouse in a tissue (kidney) selective manner. *J Biochem Mol Toxicol* 16:96–106.
Shao XM, Lopez B, Nathan D, Wilson J, Bankole E, Tumoyan H, Munoz A, Espinoza-Derout J, Hasan AM, Chang S, Du C, Sinha-Hikim AP, Lutfy K, and Friedman TC (2019) A mouse model for chronic intermittent electronic cigarette exposure exhibits nicotine pharmacokinetics resembling human vapers. *J Neurosci Methods* 326:108376
Siu EC and Tyndale RF (2007) Characterization and comparison of nicotine and cotinine metabolism in vitro and in vivo in DBA/2 and C57BL/6 mice. *Mol Pharmacol* 71:826–834.
Siu EC, Wildenauer DB, and Tyndale RF (2006) Nicotine self-administration in mice is associated with rates of nicotine inactivation by CYP2A5. *Psychopharmacology (Berl)* 184:401–408.
Su T and Ding X (2004) Regulation of the cytochrome P450 2A genes. *Toxicol Appl Pharmacol* 199:285–294.
Tseng A, Singh P, Marquez P, Hamid A, and Lutfy K (2019) The role of endogenous pituitary adenylyl cyclase activating polypeptide (PACAP) in nicotine self-administration, reward and aversion. *Pharmacol Biochem Behav* 181:46–52.
van Iersel M, Walters DG, Price RJ, Lovell DP, and Lake BG (1994) Sex and strain differences in mouse hepatic microsomal coumarin 7-hydroxylase activity. *Food Chem Toxicol* 32:387–390.
Voncken P, Rustemeier K, and Schepers G (1990) Identification of cis-3′-hydroxycotinine as a urinary nicotine metabolite. *Xenobiotica* 20:1353–1356.
Zhou X, Zhuo X, Xie F, Kluetzman K, Shu YZ, Humphreys WG, and Ding X (2010) Role of CYP2A5 in the clearance of nicotine and cotinine: insights from studies on a Cyp2a5-null mouse model. *J Pharmacol Exp Ther* 332:578–587.

Address correspondence to: Dr. Keiko Kanamori, 605 E. Huntington Dr., Suite #103, Monrovia, CA 91016. E-mail: kkanamori.hmri@gmail.com